Dihydropyridine-sensitive skeletal muscle Ca channels in polarized planar bilayers

1. Kinetics and voltage dependence of gating

Jianjie Ma,* Cecilia Mundiña-Weilenmann,‡ M. Marlene Hosey,‡ and Eduardo Ríos*

*Department of Physiology, Rush University School of Medicine; and ‡Department of Pharmacology, Northwestern University Medical School, Chicago, Illinois 60612 USA

ABSTRACT Rabbit skeletal muscle transverse tubule (T) membranes were fused with planar bilayers. Ca channel activity was studied with a "cellular" approach, using solutions that were closer to physiological than in previous studies, including asymmetric extracellular divalent ions as current carriers. The bilayer was kept polarized at −80 mV and depolarizing pulses were applied under voltage clamp. Upon depolarization the channels opened in a steeply voltage-dependent manner, and closed rapidly at the end of the pulses. The activity was characterized at the single-channel level and on macroscopic ensemble averages of test-minus-control records, using as controls the null sweeps. The open channel events had one predominant current corresponding to a conductance of 9 pS (100 mM Ba^{2+}). The open time histogram was fitted with two exponentials, with time constants of 5.8 and 30 ms (23°C). Both types of events were virtually absent at −80 mV. The average open probability (fractional open time) increased sigmoidally from 0 to a saturation level of 0.08, following a Boltzmann function centered at −25 mV and with a steepness factor of 7 mV. Ensemble averages of test-minus-control currents showed a sigmoidal activation followed by inactivation during the pulse and deactivation (closing) after the pulse. The ON time course was well fitted with "m^3h" kinetics, with τ_m = 120 ms and τ_h = 1.2 s. Deactivation was exponential with τ = 8 ms. This study demonstrates a technique for obtaining Ca channel events in lipid bilayers that are strictly voltage dependent and exhibit most of the features of the macroscopic I_{Ca}. The technique provides a useful approach for further characterization of channel properties, as exemplified in the accompanying paper, that describes the consequences on channel properties of phosphorylation by cAMP dependent protein kinase.

INTRODUCTION

Ca channels in excitable cells constitute key links in the coupling of membrane excitation to cellular effector functions. Dihydropyridine (DHP)-sensitive channels constitute a family of channels that includes the "slow" channel of skeletal muscle (Avila-Sakar et al., 1986) and the L-type or high threshold channel of heart muscle (Bean, 1989). In both of these channels, an essential component is a protein that binds dihydropyridines with high affinity. These DHP receptors are found at highest density in the transverse (T) tubular membrane of skeletal muscle (Glossman et al., 1983; Fosset et al., 1983). Consequently, skeletal muscle T membranes have served as the prototype for biochemical studies of Ca channels, and their use has allowed for the purification of the channels (reviewed in Hosey and Lazdunski, 1988; Campbell et al., 1988; Glossmann and Striessnig, 1990), cloning of their cDNA (Tanabe et al., 1987), and the demonstration of a large degree of homology between skeletal and cardiac DHP receptors, as well as with the voltage-gated Na channels (Tanabe et al., 1987; Mikami et al., 1989).

The interest in the skeletal muscle DHP receptors was enhanced by the realization that in addition to constituting the channels that carry the slow Ca current (I_{Ca}), they also serve a role as the voltage sensors that control gating of the sarcoplasmic reticulum Ca release channel in the process of excitation-contraction (EC) coupling (Ríos and Brum, 1987; Tanabe et al., 1988, 1990). Therefore, the study of the skeletal muscle DHP receptor has become attractive for both the field of EC coupling and that of voltage-gated channels in general.

The location of the DHP-sensitive Ca channels in the narrow T tubules has impeded patch clamp studies and stimulated reconstitution approaches. Isolated T membrane vesicular fractions (Rosemblatt et al., 1981; Galizzi et al., 1984; Meissner, 1984) have been fused to lipid bilayers, resulting in the incorporation of the DHP-sensitive Ca channels (Affolter and Coronado, 1985; Ma and Coronado, 1988). Purified DHP receptors from skeletal muscle have been shown to yield similar but not identical channel activities in bilayers (Flockerzi et al., 1986; Smith et al., 1987; Talvenheimo et al., 1987).

Most of the previous studies of Ca channels in bilayers have been carried out at constant membrane potential, with the channels conducting outward Ba current. These

Address correspondence to Dr. E. Ríos, 1750 West Harrison Street, Rush University School of Medicine, Chicago, IL 60612.
Dr. Mundiña-Weilenmann's permanent address is Department of Physiology and Biophysics, Facultad de Medicina, Universidad de La Plata, 60 y 120 La Plata, Argentina 3-4833.

0006-3495/91/10/890/12 $2.00

studies have defined the selectivity, permeation and pharmacological properties of the channels, but their conditions are far removed from the normal physiological gating of the channels under changing membrane potential.

The present two papers describe studies of Ca channels from T membrane vesicles of rabbit skeletal muscle fused with planar bilayers. In these studies we took a "cellular" approach, that originated in the previous work of Rosenberg et al. (1986, 1988) on cardiac channels and of Mejía-Alvarez et al. (1991) on skeletal muscle channels. As in their work, we kept the bilayer polarized at a negative potential, which in our case was close to a normal resting potential, and pulsed it as one would pulse a cell under voltage clamp. This approach led to the observation of voltage-activated currents, which we processed as regular whole cell data, including subtraction of "controls" to eliminate capacitive currents, and construction of ensemble averages to study macroscopic kinetics. In addition, we used ionic solutions for our recording conditions that were closer to physiological than in previous work; in particular, the current-carrying ion (Ba^{2+}) was present in the *trans* or extracellular compartment only, so that the channels would conduct an inward current. We tried to reduce to a minimum (but could not eliminate altogether) the use of the dihydropyridine agonist Bay K 8644 in the recording solutions. The result of this approach was an improved description of the voltage dependence and kinetics of activation, inactivation and deactivation of Ca channels, at both the single channel and macroscopic level.

METHODS

Preparation of transverse tubule membranes

Transverse tubule membranes were isolated from frozen rabbit skeletal muscle tissue, according to the procedure of Galizzi et al. (1984). Membranes were stored in liquid nitrogen at a concentration of 5–7 mg/ml of protein in 20 mM Tris-HCl buffer at pH 7.4. The T membrane fraction contained 30–70 pmol DHP receptor/mg protein, measured by the binding of (+)[^{3}H]PN200-110 (Amersham Corp., Arlington Heights, Illinois).

Bilayer reconstitution and single channel recording

Planar bilayers were formed following the Müeller-Rudin procedure. The membranes were painted with a 1:1:0.2 mixture of phosphatidylethanolamine, phosphatidylserine and cholesterol (Avanti Polar Lipids, Birmingham, AL) dissolved in decane (Aldrich Chemical Co., Milwaukee, WI) at a concentration of 50 mg lipid/ml. The concentration of cholesterol used was critical to the stability of the membranes when steadily polarized. Membranes with cholesterol below 0.2 were unstable at −80 mV, and those with >0.3 cholesterol were stable but showed no vesicle fusion.

A suspension of T membranes (2–3 μl) was added to the solution in the *cis* compartment. The "internal" solution, present in the *cis* compartment, contained 200 mM KCl, 10 mM HEPES-Tris, 3 mM $MgATP^{2-}$ and 0.3 μM Bay K 8644 (titrated to pH = 7.4 with Tris base). The concentration of the DHP agonist used was the minimum that resulted in consistently measurable activity. Channels were first incorporated into the bilayer with a 200 mM KCl/50 mM NaCl (*cis-trans*) gradient. In addition, the *trans* solution contained 10 mM Hepes-Tris (pH 7.4). After the channels were incorporated, 100 mM $BaCl_2$ was added to the *trans* solution. The experiments were conducted at room temperature (22–24°C).

Single channel currents were recorded and voltage control was imposed with a commercial patch clamp unit (Axopatch 1C, Axon Instruments, Foster City, CA). Pulses were generated and data acquired in real time with an AT-compatible computer (CompuAdd Corp., Austin, TX, model 386/25) equipped with an A/D-D/A converter board (Labmaster DMA-100, Scientific Solutions, Solon, OH). The current was filtered at a cut-off frequency of 100 Hz with a 8-pole Bessel filter (902 LPF, Frequency Devices, Haverhill, MA), digitized at 500 Hz and stored for analysis.

Study of voltage dependence

The overall goal of this work was to describe the voltage-dependent gating of the skeletal muscle DHP-sensitive Ca channel in bilayers. To this end, the bilayers were steadily polarized at −80 mV *cis-trans* (the holding potential -h.p.-) and depolarized to various test potentials with pulses of variable duration. Fig. 1 shows a 1 s pulse to −20 mV (*a*) and the total current (*b*) recorded at a gain of 100 mV/pA in the headstage of the clamp amplifier. The record shown is representative of records obtained after partial cancellation of the large capacitative transient, which was accomplished by adding, at the input of the amplifier, the current driven by the command pulse through a 10 pF capacitor and an adjustable series resistance. As shown, this analog subtraction could reduce the early transient to less than 30 pA, which avoided saturation at the headstage.

Trace *c* in Fig. 1 shows the same current acquired, with a slightly different capacitance compensation, after amplification by a factor of 10 in a second stage. Open channel events became visible and the A/D saturated for 6–16 ms, depending on pulse amplitude, during both the ON and OFF transients. In addition to a large fast phase, the current transient had slower decaying phases, detectable for one second or longer, that were due to electrostriction (Alvarez and Latorre, 1978). These components were subtracted from the total current using a "control" current that had only capacitive and electrostrictive contributions. Controls were constructed by averaging null sweeps (like *trace d* in Fig. 1) as first described in the bilayer experiments of Rosenberg et al. (1986). All nulls in a given series of pulses to the same voltage were averaged and the average was subtracted from the total current without further processing. The difference "test-minus-control" (Fig. 1, *record e*) represents ionic current. The dihydropyridine nitrendipine (20 μM) added to the *trans* side consistently blocked these events (*record f*).

Single channel and macroscopic processing

The ionic currents, obtained as described, were subjected to conventional single channel analysis, carried out using the PCLAMP software

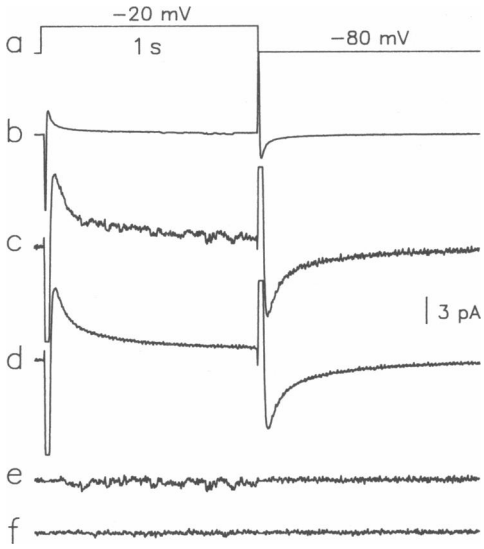

FIGURE 1 Recording of the DHP-sensitive Ca channel from skeletal muscle. Channel openings were elicited by a depolarizing pulse (−20 mV) from h.p. = −80 mV (*a*). The corresponding "test" currents were recorded at a gain of 100 mV/pA in the headstage amplifier (*b*), or multiplied by 10 in a second stage (*c*). Capacitance compensation reduced and delayed the early capacitance transient, thus preventing saturation of the headstage amplifier. The A/D converter saturated for 6–16 ms in (*c*). Null sweeps at the same test pulse were averaged to construct the "control" (*d*). Subtraction of control (*d*) from test (*c*) revealed the unitary inward channel openings (*e*). Channel events were always blocked by 20 μM nitrendipine added to the *trans* solution (*f*).

system (Axon Instruments, Foster City, CA) and custom programs. The analysis started with amplitude histograms, leading to the determination of the mean current and conductance of a predominant open state. Once the average open channel current was determined, opening and closing transitions were detected, using as threshold criterion a level equal to 0.5 of the predominant open channel current. This was followed by determination of event durations, construction of open time histograms, and computation of open probability ($\bar{P}_0$) as the fraction of the total pulse duration occupied by open events. When two open events superimposed their currents, their durations were independently added for calculation of $\bar{P}_0$. This computation of $\bar{P}_0$ was carried out on channels that were not in steady state; it is really an average of a time-dependent P_0. An analysis of its meaning will be presented in the Discussion.

In addition to single channel analysis, ensembles of ionic currents obtained with pulses to the same voltage were averaged. Typically, one stable channel in a bilayer could be subjected to between 50 and 300 pulses, covering from one to five different test voltages. From 50 to 150 sweeps were obtained per voltage level, per bilayer. The ensemble averages shown were the result of averaging 5 to 10 such experiments together (250–500 sweeps).

The voltage dependence of channel open probability and the time dependence of averaged currents were fitted with theoretical functions using nonlinear least-squares routines (Scarborough, 1966) that also calculated a standard error of the parameter estimates (Cleland, 1977).

RESULTS

Voltage-dependent activation of T membrane Ca channels in bilayers

Fig. 1*c* shows the total current during a pulse from h.p. (−80 mV) to −20 mV, and trace *e* shows the corresponding ionic current. The membrane was silent before the pulse (even though the driving force for inward Ba^{2+} movement was greatest at h.p.); active gating of the channel became visible shortly after the beginning of the pulse, and the activity ceased abruptly upon repolarization. Fig. 2 shows representative sweeps, during 2 s pulses to various voltages (listed at left in millivolts). Channel openings were observed at potentials above −40 mV. Beyond this threshold, the open probability increased with voltage. It is also visible in the records of Fig. 2 that channel activity was greatest during the first half of the 2 s pulse, then decayed. This inactivation will be obvious in ensemble averages presented later.

A plot of $\bar{P}_0$ vs. voltage of the test pulse (V) was constructed (Fig. 3). Average values of individual symbols in panel *A* represent average values over 16 to 32 sweeps, obtained on the same bilayer, at the voltage in the abscissa. The different symbols correspond to data obtained from different bilayers. In all cases, the voltage dependence of channel opening was sigmoidal, with a well defined threshold ~ −40 mV and saturation above 0 mV. The values at the same voltage were averaged and represented (± one std. deviation) in panel *B*. These

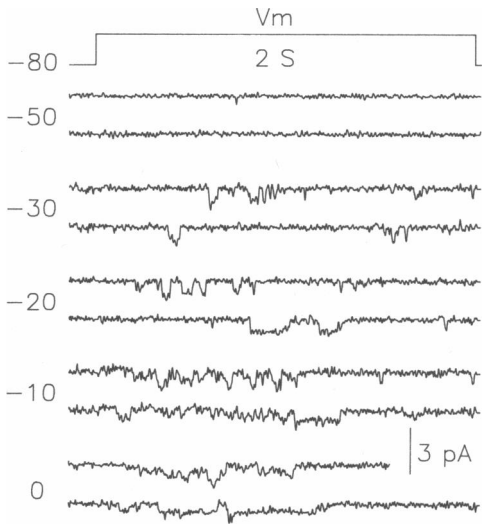

FIGURE 2 Voltage dependence of the Ca channel in the bilayer. Representative "test-minus-control" records at different membrane potentials (listed in mV) were taken from one bilayer experiment. Unless otherwise indicated, currents were filtered at 100 Hz and digitized at a rate of 0.5 kHz.

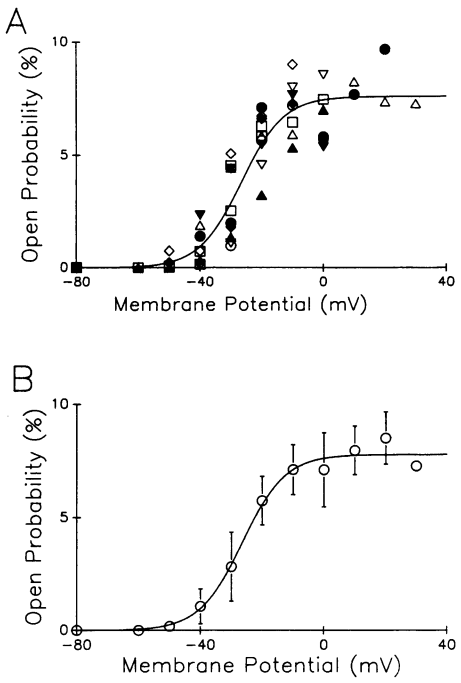

FIGURE 3 Open probability as a function of membrane potential. (*A*) Individual symbols represent values of the open probability $\overline{P}_0$, computed as described in Methods. The different types of symbols represent data from 10 different experiments. (*B*) Data points are averages of 10 experiments (represented in *A*). Vertical bars indicate standard deviation. The curve represents the best fit Boltzmann distribution function (Eq. 1), with the following parameters: transition potential $\overline{V}$ = −26.36 (0.17) mV, steepness factor K = 6.98 (0.15) mV, and maximum open probability $\overline{P}_{max}$ = 0.078 (0.008) %.

averages were fitted with a "Boltzmann" function of voltage:

$$\overline{P}_0 = \overline{P}_{max} \frac{1}{1 + e^{-(V-\overline{V})/K}}, \quad (1)$$

where $\overline{P}_{max}$ is the maximum value of $\overline{P}_0$, $\overline{V}$ is the transition or midpoint voltage and K is the steepness factor. The smooth line shown in Fig. 3 was generated with the best fit. Its parameters are $\overline{P}_{max}$ = 0.078 (0.008), $\overline{V}$ = −26.4 (0.2) mV and K = 7.0 (0.1) mV. In most cases, function (1) could also be fitted to data from individual bilayers. The best fit parameters for 10 individual bilayers are listed in Table 1; they are similar to the collectively fitted parameters.

Single channel conductance and open time distribution

Amplitude histograms constructed from 32 sweeps on the same bilayer, with pulses to −20 and 0 mV, are depicted in Fig. 4. The histograms at −20 and 0 mV were

TABLE 1 **Voltage dependence of channel opening from individual experiments**

Bilayer no.	$\overline{P}_{max}$	$\overline{V}$	K
		mV	*mV*
1	0.071	−27.7	5.6
2	0.079	−16.6	8.3
3	0.077	−26.9	3.4
4	0.072	−32.1	9.5
5	0.087	−20.6	4.6
8	0.082	−29.7	9.1
10	0.111	−25.0	8.9
Average of fits	0.083 ± 0.01	−25.5 ± 5.0	6.9 ± 2.4
Fit to averages	0.078 ± 0.01	−26.4 ± 0.2	7.0 ± 0.2

Time-averaged open probability values, obtained at different voltages in individual bilayers were fitted with Eq. 1. The data from bilayers 6, 7, and 9 could not be fitted individually but were included in the cumulative fit. The row labeled "average of fits" lists averages of seven individual best fit parameter values (± standard deviation). The last row "fit to averages" lists the best fit values for averaged data over all 10 bilayer experiments.

fitted as the sum of two gaussian functions. The best-fit theoretical curves, represented in the figure, describe the data well (the large bin at amplitude zero corresponds to the several milliseconds of saturation at the beginning of the pulse).

A central value of the open channel current is well defined at both voltages. The value of the mean of the gaussian that describes open channel intensities was 0.46 pA at 0 mV and 0.63 at −20 mV. The corresponding slope conductance is 9 pS. The conductance derived from these distributions is equal to one of the two higher conductance levels (9 and 12 pS) described by Ma and

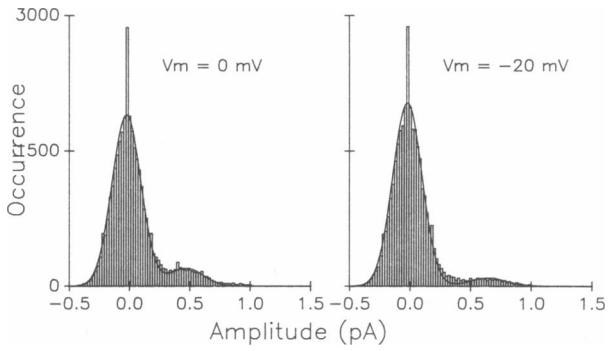

FIGURE 4 Current amplitude histogram at 0 and −20 mV. Each histogram was constructed from 32 consecutive test-minus-control records. The superimposed curves represent the best fit Gaussian distributions. Baseline noise had a central value (μ_n) = −0.03 pA and standard deviation (σ_n) = 0.12 pA at both voltages. The parameters of open channel currents were: μ = 0.46 pA and σ = 0.14 pA at 0 mV; μ = 0.63 pA and σ = 0.15 pA at −20 mV. The large bin at 0 pA corresponds to the brief initial period of saturation.

Coronado (1988); the currents in the present experiments probably include events at both levels.

The histogram of amplitudes also gives information on the noise characteristics of these records. The standard deviation of the noise, σ_n, can be obtained from the gaussian fits to the baseline component (centered at 0) in the amplitude histograms. It can also be obtained from amplitude histograms at −50 mV, and is typically 0.12 pA in these experiments.

The histogram of open times calculated from 192 sweeps, with 2-s pulses to −10 mV, is shown in Fig. 5 *A*. The bin interval in the histogram is equal to the sampling interval, 2 ms. A total of 6,620 open events were detected. The dead time of the recording system, estimated as 0.5 × the rise time of the Bessel filter stage, was ~1.8 ms. Therefore, the first bin in the histogram, corresponding to the interval 0–2 ms, was not represented in the figure. The histogram at −10 mV was fit as the sum of two exponentials

$$y = (W_1/\tau_1)e^{-t/\tau_1} + (W_2/\tau_2)e^{-t/\tau_2}, \quad (2)$$

of time constants τ_1 and τ_2, where W_1 and W_2 are the total numbers of events characterized by time constants τ_1 and τ_2. The best fit parameters were W_1 = 16,350, τ_1 = 5.8 ms, W_2 = 2,068, τ_2 = 30 ms. This fit was better than a single exponential ($p < 0.03$), based on a likelihood ratio statistic of 10.6 (Hui and Chandler, 1990; Bickel and Doksum, 1977). The two time constants were different from the dwell times that have been previously observed in bilayer-fused Ca channels; reasons for the apparent discrepancy will be considered in the Discussion.

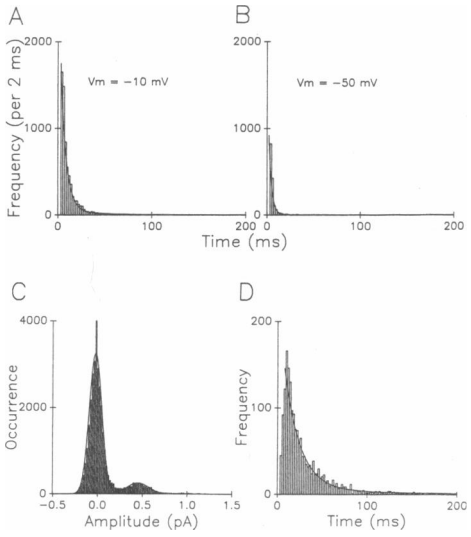

FIGURE 5 Effects of digital filtering on the open time distribution. (*A*) Channel open times at −10 mV were calculated from 192 episodes, as in Fig. 2. A total of 6,620 open events were detected with a threshold setting (φ) of 0.3 pA (cf Discussion). The solid line represents the best fit as a sum of two exponentials: (Eq. 2), where W_1 = 16,350, τ_1 = 5.8 ms; W_2 = 2068, τ_2 = 30 ms. (*B*) Open events at −50 mV calculated from 80 episodes. A total of 636 events were detected. The histogram was scaled by a factor of 2.4 (192/80), for direct comparison with (*A*). A single exponential decay was used to fit the data: W = 5,352, τ = 3.0 ms. (*C*) Amplitude histogram, after digitally filtering at 30 Hz the current records used in Fig. 4 (0 mV). The baseline and open channel amplitude distribution changed. The corresponding Gaussian distributions had the following parameters: μ_n = −0.03 pA, σ_n = 0.07 pA; μ = 0.44 pA, σ = 0.12 pA. (*D*) Open time histogram after digital filtering at 30 Hz. A total of 1,821 open events were detected with the same 192 episodes, as in *A*. The histogram was fitted with a sum of two exponential distributions of parameters: W_1 = 3,780, τ_1 = 17.3 ms; W_2 = 776, τ_2 = 92.5 ms.

In contrast to the data obtained with pulses to −10 mV (Fig. 5 *A*), only 636 events were detected in 80 sweeps at −50 mV. Fig. 5 *B* represents the histogram of open times (the values were normalized to the same total recording interval to make both histograms directly comparable). The histogram at −50 mV was fit as one exponential decay, with amplitude W = 2230 and time constant τ = 3.0 ms. It is likely that these are false events due to noise (cf Discussion). The value of W per unit time at −50 mV (14 s^{-1}) is significantly smaller than the value of W_1 per unit time at −10 mV (43 s^{-1}), indicating the existence of voltage-dependent openings of both 5 and 30 ms dwell times at −10 mV. In this interpretation, the ratio 14/43 = 0.33, gives the fraction of false detections of short openings at −10 mV.

Voltge-dependent openings longer than 100 ms were also found, but with very low probability, and the goodness of fit of the open time histogram was not improved with three exponentials. Because such long openings have been described in studies at steady voltages (Ma and Coronado, 1988), as well as using voltage pulses (Mejía-Alvarez et al. 1991), we asked whether our data could be made consistent with such long events. To that end we filtered digitally the records at a frequency of 30 Hz, similar to the filtering used by Mejía-Alvarez et al. (1991) and slightly lower than used by Ma and Coronado (1988) and constructed amplitude histograms and open time histograms of the filtered records (Fig. 5, *C* and *D*). The open time histogram changed substantially after digital filtering: as expected with the longer dead time, a majority of the openings at 6 ms and below were lost; more importantly, a large number of openings longer than 50 ms appeared. The histogram of the filtered records was fit best with W_2 = 3,780, τ_2 = 17 ms, W_3 = 776 and τ_3 = 92 ms. It is likely that the latter time constant is actually describing brief bursts of openings, separated by narrow gaps that go unnoticed with the heavier filtering. We cannot, however, rule out the possibility that such long open times do

exist, and are lost at the greater bandwidth because of false *closing* events due to noise.

Kinetics of gating. Activation, inactivation and deactivation

As described recently, voltage-dependent DHP-sensitive channels fused with bilayers inactivate after opening (Mejía-Alvarez et al., 1991). A sequence of ionic current records, obtained with 5-s pulses to −10 mV is shown in Fig. 6. In all cases, the stimulus resulted in openings that clustered early in the pulse and disappeared by the end of the depolarization. This was the case at −20 mV and greater voltages, indicating that inactivation was essentially complete at voltages that caused appreciable channel opening. This qualitative observation is used below in a specific description of the time dependence of channel gating.

Fusion of vesicles with bilayers usually resulted in the incorporation of more than one channel, as suggested by the superimposed open events of the same amplitude, visible for instance in Fig. 6. Though infrequent, double openings were observed in virtually all bilayers. By contrast, triple openings were detected by the software extremely infrequently and were seldom convincing to the eye. Accordingly, for analyses that required the number N of functional channels in the bilayer, we used two or three as estimates.

Fig. 7 *A* shows 10 records of ionic current, obtained in succession, with 2 s pulses to −10 mV, separated by intervals of 5 s. The ensemble average (Fig. 7 *B*) was obtained with 312 sweeps like the ones in *A*, in 12 different bilayers. To minimize noise, null sweeps were

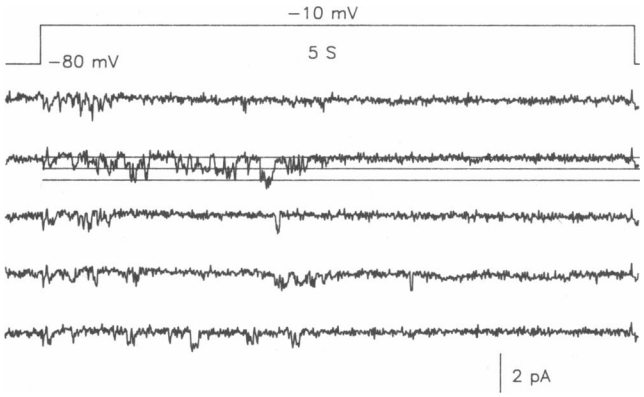

FIGURE 6 The channels inactivate completely during a 5s depolarizing pulse. The episodes represented were obtained consecutively, with 5s pulses, at 7 s intervals. The digitization rate was 0.2 kHz. The horizontal lines on the second episode were traced at −0.55 pA and −1.1 pA, corresponding to one and two average amplitudes of the channel current.

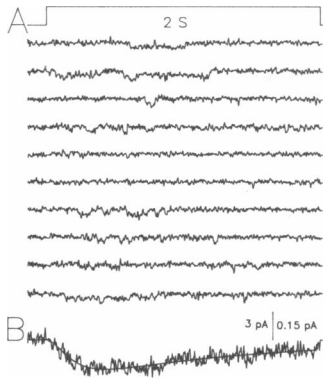

FIGURE 7 Ensemble averages of channel currents at −10 mV. (*A*) Single channel currents upon pulsing to −10 mV from a holding potential of −80 mV. Episodes shown are consecutive, obtained at 5 s intervals. (*B*) Ensemble average of 312 episodes obtained in 12 experiments like *A*, null sweeps were excluded. The solid line is the best fit with Eq. 6. Best fit parameters are I_{max} = 0.25 (0.004) pA, τ_m = 118 (3.6) ms, and τ_h = 1.24 (0.1) s.

excluded from the average. Such an ensemble average with nulls excluded will be represented as $\langle I(t, V)\rangle^*$ (a regular ensemble average will be $\langle I(t, V)\rangle$). The vertical bar corresponds to 3 pA in the ionic current records or 0.15 pA in $\langle I(t, V)\rangle^*$ (because 25% of all sweeps were nulls (cf Table 2), the vertical bar would correspond to 0.113 pA if the record represented a regular average).

A quantitative description of the time course of gating is represented by the continuous line in Fig. 7 *B*. The curve was generated with the equation

$$\langle I(t, V)\rangle^* = A[m(t)]^3 h(t), \tag{3}$$

where $m(t)$ and $h(t)$ are first order activation and inactivation variables defined as

$$m(t) = m(\infty)[1 - \exp(-t/\tau_m)], \tag{4}$$

and

$$h(t) = h(\infty) + [h(0) - h(\infty)] \exp(-t/\tau_h). \tag{5}$$

This function was fitted to the ensemble average by a least squares routine, with adjustable parameters τ_m, τ_h and a scaling factor $Am^3(\infty)h(0)$ ($\equiv I_{max}$). $h(\infty)$ was sometimes fitted by the program, but it was set to 0 for pulses to −20 mV and higher voltages, based on the observation that the open probability essentially decayed to 0 after 5 s (Fig. 6). This approximation was made for the actual fit in Fig. 7 *B*. Another simplification resulted from using the ensemble average with nulls excluded. It will be shown in the Discussion that excluding nulls from the average is equivalent to making $h(0)$ = 1 in Eq. 5. Therefore, a simplified representation of the

ensemble average is

$$\langle I(t,V)\rangle^* \simeq I_{max}[1 - \exp(-t/\tau_m)]^3 \exp(-t/\tau_h). \quad (6)$$

and $I_{max} = A\,m^3(\infty)$.

The best fit represented by the continuous curve (Fig. 7 *B*) was obtained with I_{max} = 0.25 (0.06) pA, τ_m = 118 (3.6) ms and τ_h = 1.2 (0.1) s. When $h(\infty)$ was allowed to vary, the program determined values between −0.1 and 0.2 without significantly improving the fit.

The range of voltages in which this formal description of the kinetics of channel activation and inactivation was possible, was restricted to between −20 and 0 mV. Due to the low open probability, it was not possible to obtain a meaningful fit to the ensemble average at −30 mV. The currents became too small at potentials above 0 mV. The averaging and fitting procedure was repeated at potentials of −20, −10, and 0 mV. Table 2 lists the average values of fits to data from different individual bilayers. The results show that the "m^3h" description is adequate. In the voltage range studied the activation time constant was strongly voltage dependent, whereas the inactivation time constant was not.

Further experiments were designed to examine the kinetics of channel closing or deactivation at the OFF of the pulse. Traces of ionic currents analyzed for this purpose are shown in Fig. 8 *A*. To improve the resolution of the closing phenomenon, a greater sampling frequency was used (4 points/ms). The pulse duration was reduced to 400 ms, to maximize the activity at the end of the pulse. Additionally, the second amplification stage was eliminated, to avoid saturation of the A/D converter. The OFF of the ensemble average (Fig. 8 *B*) was fitted with a single exponential decay to zero. The fitted interval started 10 ms after the end of the pulse, to skip the group delay of the 0.1 kHz Bessel filter. The best fit time constant was 8 (1.4) ms for the average shown. This is the first time that the kinetics of closing of these channels have been resolved in single channel experiments.

TABLE 2 Voltage dependence of kinetic parameters

Voltage	τ_m	τ_h	I_{max}	M_0/M	n
mV	ms	s	pA		
0	100 ± 3	1.54 ± 0.04	0.223 ± 0.004	0.22 ± .02	5
−10	118 ± 4	1.24 ± 0.04	0.245 ± 0.006	0.25 ± .03	12
−20	137 ± 5	1.44 ± 0.06	0.157 ± 0.005	0.30 ± .02	11

Ensemble averaged currents at each membrane potential were fitted according to: $I = I_{max}(1 - e^{-t/\tau_m})^3 e^{-t/\tau_h}$. Numbers given for τ_m, τ_h, and I_{max} are best fits ± standard deviations. M_0/M = number of null sweeps/total number of sweeps (mean value ± standard error of the mean). n = number of experiments for each condition.

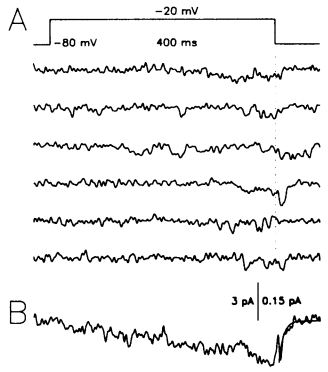

FIGURE 8 Channel closing (deactivation) at the end of the pulse. (*A*) Selected records are consecutive episodes of 500 ms, recorded at a total gain of 100 mV/pA. The digitization rate was 4 kHz. (*B*) Ensemble average of 110 episodes as in *A*, from four bilayers, with null episodes excluded. The bar corresponds to 3 pA in the individual records or 0.15 pA in the averages. An average with nulls included would be 25% smaller. The droop seen in the ensemble average immediately after repolarization probably corresponds to a nonlinearity in the response of the system at the peak of the current transient, leading to imperfect cancellation of test and control. The OFF portion was fitted starting 10 ms after the trailing edge of the pulse, by a single exponential decay, with τ = 8 (1.2) ms.

Availability of the channel to open

The fifth column in Table 2 lists the percentage M_0/M of null sweeps. The entries in the column are averages of separate determinations in several different bilayers (± standard errors of the mean). The number of bilayers averaged at each voltage is listed as column 6. The number of null sweeps was slightly voltage dependent, varying between 22.4% at 0 mV and 29.7% at −20 mV; the difference was significant. The technical importance of the existence of nulls has been noted in Methods -they allow us to have controls-. Their relationship with the occupancy of inactivated states will be considered in the Discussion.

DISCUSSION

The aim of the present work was to characterize the voltage-dependence of the skeletal muscle Ca channels, in terms suitable for comparison with the properties of I_{C_a} and EC coupling events, as derived from whole cell studies. Accordingly, we devised conditions comparable to experiments in whole cells. As in two previous studies (Rosenberg et al., 1986, 1988; Mejía-Alvarez et al., 1991) the bilayers were held at a negative potential, pulsed, and the current records analyzed using nulls as controls. In the present experiments we attempted to use conditions closer to those encountered physiologically. Thus,

ATP and Mg^{2+} were present in the *cis* side, the current carrier, Ba^{2+}, was present only in the "extracellular" solution, so that the open channel conducted inward current at the voltages applied here, and asymmetric ionic solutions were used with high 'internal' K and 'external' Na. As in previous studies, we found the need to use the DHP agonist BAY K 8644 to help induce channel opening. We found that 0.3 μM was the lowest concentration that allowed for consistent observation of "workable" channel activity. This concentration is 3–10-fold lower than that used in previous studies.

The channel activity observed with this technique had a voltage dependence that was both steep and strict. Channels that did not open unless the membrane was pulsed were observed in 110 out of 124 experiments; the data shown in this paper are representative of those 110 experiments. In the other 14 experiments, we observed channel activity that did not inactivate (channel activity was present in steadily depolarized membranes) and apparently had no voltage dependence because the channels were open even at −80 mV. These results confirm the observation of Mejía-Alvarez et al. (1991), who described both voltage-dependent and independent Ca channels in bilayer recordings of skeletal muscle T membranes. In the present study, however, voltage-independent channels were found with much lower frequency (11% vs. about 54% in the study cited). By conducting all our experiments at a holding potential of −80 mV we could easily separate the two groups and concentrate on the inactivating, voltage-dependent population.

The durations of the open events recorded here are smaller than in previous studies with T membranes in bilayers, in which "short" openings of ~25 ms and "long" events of ~150 ms were consistently found (Affolter and Coronado, 1985; Ma and Coronado, 1988; Mejia-Alvarez et al., 1991). Of the two characteristic open times, 5.8 and 30 ms, detected in the present study, it is likely that the longer one corresponds to the short time constant of previous studies. The shorter openings are a new observation; these openings were defined using as threshold (φ) one half of the open event current (or 0.3 pA), and all events were included, regardless of duration. With this criterion, false events will be detected, at a rate that can be predicted from the ratio φ/σ_n (2.7 in our case) and knowledge of the noise spectrum. According to Colquhoun and Sigworth (1983, Fig. 11.5), a rate of false events of between 15 s^{-1} and 25 s^{-1} can be predicted for a $\varphi/\sigma_n = 2.7$. In the present experiments the rate of short openings was $\simeq 43$ s^{-1} at −10 mV and $\simeq 14$ s^{-1} at −50 mV. It is reasonable to believe that the short openings at −50 mV were false events and that the extra events detected at −10 mV corresponded to actual voltage-dependent channel openings. The reason that these openings went undetected in previous studies at steady voltages may be that they are absent under conditions in which only non-inactivating channels are detected. In the study of Mejía-Alvarez et al. (1991) the sampling rate (100/s) and filtering used (30 Hz) probably left these brief openings undetected.

Voltage-dependence of channel activity

The voltage dependence observed in a majority of bilayers in the present study was quantified in two ways: in the $\overline{P}_0$ vs. V curves of Fig. 3 and Table 1, and in the voltage dependence of the parameters obtained from fits to the ensemble averages (Fig. 7 and Table 2). The first description is a microscopic one, in that it can only be derived from single channel currents. The second is macroscopic and should be directly comparable with the corresponding description of whole cell current. In the following we recall or derive formulas linking the microscopic and macroscopic descriptions.

The relationship between the voltage- and time-dependent open channel probability $P_0(t, V)$ and the current averaged over the ensemble of sweeps at voltage V is

$$P_0(t, V) = \langle I(t, V)\rangle/(N\,i), \tag{7}$$

where N is the number of active channels in the bilayer and i is the single channel current. Instead of the ensemble average $\langle I(t, V)\rangle$, we compute the average currents with nulls excluded ($\langle I(t, V)\rangle^*$). In terms of this function the open probability is:

$$P_0(t, V) = \langle I(t, V)\rangle^* \frac{M - M_0}{MN\,i} \tag{8}$$

where M is the total number of sweeps and M_0 is the number of null sweeps.

Fitting the macroscopic ensemble current with function (3) is equivalent to assuming that the voltage- and time-dependence of the individual channel gating is of the form

$$P_0(t, V) = P_{max}\, m^3(V, V_0, t)\, h(V, V_0, t), \tag{9}$$

where P_{max} is the absolute maximum of the open probability, attained when m and h equal 1.

Substituting m^3h from Eq. 3 into Eq. 9,

$$P_0(t, V) = \langle I(t, V)\rangle^* P_{max}/A. \tag{10}$$

From Eqs. 7 and 10 we derive the equivalence

$$P_{max} = A/(N\,i) = I_{max}/[m^3(\infty)\,N\,i]. \tag{11}$$

Eq. 11 expresses a relationship between the micro-

scopic and the macroscopic parameters, and amounts to a practical recipe for obtaining P_{max}: it is the ratio between the fitted parameter I_{max} and the individual channel current, at voltages sufficiently high for maximal activation ($m(\infty) = 1$) and normalized per channel. This correspondence does not depend on the details of the expression used for describing activation (it could be other than m^3).

The correspondence between the macroscopic description of gating, embodied in Eq. 6, and gating at the single channel level, can now be summarized. The variables m and h describe directly gating at the channel level. The scaling parameter I_{max} expresses the voltage dependence of activation (it is proportional to $m^3[\infty]$) and is also proportional to the microscopic parameter P_{max}, the absolute maximum of the open channel probability.

With these relationships we may now understand the implications of one of the most interesting results of the present experiments, namely, that full activation by voltage does not correspond to full opening of the individual channels. Moreover, the open probability of a fully activated, fully available channel, P_{max} in Eq. 9, is very small. Indeed, from Eq. 11 and the values $I_{max} = 0.25$ pA (Table 2), $i = 0.55$ pA and $N = 2$ or 3 (Fig. 6), $P_{max} \simeq 0.18$. One way of interpreting Eq. 9 is that the channel has two gates in series: one is opened by voltage, its open probability, spanning the range 0 to 1, is expressed by m^3h; the other opens and closes independently, its open probability is P_{max}.

The P_{max} obtained here is much lower than corresponding quantifiers of open probability in previous bilayer experiments with cardiac (P_{max} was close to 1, Rosenberg et al. 1988), and skeletal muscle channels. The low P_{max} we observed may be due to our use of a 3 to 10-fold lower concentration of Bay K 8644. In the two-gate interpretation proposed above, Bay K would be acting on the voltage-independent gate.

The low value of P_0 has another interesting consequence. Skeletal muscle Ca^{2+} currents are small when compared with the density of DHP receptors. This has prompted the speculation that only a small fraction of the DHP receptors constitute functional current carrying channels (Schwartz et al., 1985). In this view, the majority would perform as voltage sensors of EC coupling and only a small proportion would constitute functional channels, i.e., those that can be activated to a high value of P_0. However, we show in the present studies that P_0 is very low even when the channels are maximally activated by voltage. The maximum P_0 actually attainable at large depolarizations is $< P_{max}$ because of inactivation. This suggests that the small amplitude of macroscopic Ca^{2+} currents of skeletal muscle may simply be a consequence of the tendency of even functional channels, fully activated by voltage, to stay closed most of the time (as proposed by Lamb and Walsh, 1987).

The $\overline{P}_0$ vs. V curve of Fig. 3 constitutes an alternative quantification of voltage dependence. $\overline{P}_0$ is defined in Methods as the fractional open time during the pulses, and includes multiple openings when multiple channels are present. It is then a time-averaged open probability, multiplied by the number of functional channels in the bilayer

$$\overline{P}_0(V) = (N/T) \int_0^T P_0(t, V)\, dt, \tag{12}$$

where T is the pulse duration. Introducing the expression (9) for $P_0(t, V)$ in (12)

$$\overline{P}_0(V) = N P_{max} \int_0^T m^3(\infty, V)\, h(0)[1 - e^{-t/\tau_m}]^3 e^{-t/\tau_h}\, dt/T, \tag{13}$$

and for $T \gg \tau_m$

$$\overline{P}_0(V) = N P_{max}\, m^3(\infty, V)\, h(0)\, \beta, \tag{14}$$

where $\beta \equiv (1 - e^{-T/\tau_h})\, \tau_h/T$.

Because τ_h and β are essentially independent of voltage (Table 2) and $h(0)$ is a function of the holding potential, $\overline{P}_0$ is proportional to $m^3(\infty, V)$; its voltage dependence, represented in Fig. 3 and Table 1, only expresses the steady-state voltage dependence of the activation variable. From Eq. 1, $\overline{P}_0$ tends to $\overline{P}_{max}$ at high voltages, thus an expression for $\overline{P}_{max}$ can be obtained from Eq. 14 at high voltages

$$\overline{P}_{max} = N\, h(0)\, \beta\, P_{max}. \tag{15}$$

This expression allows for another determination of P_{max}. It will be applied for a 2-s pulse, with $\tau_h = 1.24$ s, $\beta = 0.5$, assuming again that N is 2 or 3. The parameter $h(0)$ can be estimated from the fraction of null sweeps (Cavalié et al., 1986) as

$$M_0/M = [1 - h(0)]^N. \tag{16}$$

Because $M_0/M \simeq 0.25$, $h(0) \simeq 0.43$. Therefore, the value of P_{max} should be ~ 0.15, consistent with the previous estimate.

Comparison with Ca currents in whole cells

The kinetic properties of the Ca channels in the present bilayer study compare well with those of whole cell Ca or Ba currents. Thus, I_{Ca} activates and inactivates slowly in skeletal muscle (Almers and Palade, 1981; Donaldson and Beam, 1983) following in frog an m^3h dependence (Sánchez and Stefani, 1983) with τ_m between 50 and 200 ms, depending on membrane potential and tempera-

ture. This range is consistent with the value of 118 ms reported here.

A recent reexamination of the nature of inactivation of I_{Ca} on intact and cut frog skeletal fibers (Cota and Stefani, 1989; Francini and Stefani, 1989) has established the existence of a voltage-dependent mechanism of inactivation, that does not depend on the divalent cation species carrying the current, and is distinct from a depletion mechanism which becomes dominant in special circumstances (Almers et al., 1981; Francini and Stefani, 1989). The agreement of the inactivation time constant measured here (1.3 s) with the whole cell values is striking. The time constant of inactivation is close to 1.3 s in intact frog fibers at −10 mV and 23°C (Cota and Stefani, 1989), it is mildly voltage dependent between −20 and 20 mV (Francini and Stefani, 1989) and is not changed essentially by substituting Ba^{2+} for Ca^{2+} as the current carrier (Cota and Stefani, 1989). Because the current carrier in the present study is Ba^{2+}, our results are consistent with the view that the Ca channels inactivate through a voltage-dependent mechanism not requiring Ca^{2+}. Of course our studies do not rule out depletion as a cause of decay of I_{Ca}.

The present currents are also similar to macroscopic I_{Ca} in the kinetics of deactivation. The I_{Ca} tails at −90 mV were reported to deactivate with an exponential time course, with a time constant of 9.2 ms in frog fibers at room temperature (Sánchez and Stefani, 1983). A similar time constant can be extracted from published records of tail current in rat muscle fibers (Mejía-Alvarez et al., 1991), although a precise value cannot be obtained without correction of the tails for nonlinear charge movement.

The present measurements were carried out with the agonist Bay K 8644 in the recording solution. Considering that Bay K induces significant changes in the gating properties of cardiac Ca channels (Hess et al., 1984; Kokubun and Reuter, 1984; Sanguinetti et al., 1986; Bechem and Schramm, 1988; Markwardt and Nilius, 1988), our results ought to be compared with measurements of I_{Ca} in skeletal muscle exposed to Bay K. However, the only systematic studies on kinetic effects of Bay K in skeletal muscle, carried out by Cognard et al. (1986) on cultured cells, did not show significant changes in activation or inactivation (they revealed as main effect a reduction in the rate of relaxation of tail currents). Therefore, activation and inactivation kinetics measured in the present experiments appear to fall within normal ranges for both reference and Bay K treated skeletal muscle cells.

In the present work, the dependence $\overline{P}_0$ vs. V was well described by a Boltzmann function of voltage, with central voltage $\overline{V} = -26$ mV and steepness factor $K = 7$ mV. This voltage dependence is reasonably consistent with that of I_{Ca} in whole cells. I_{Ca} activates with central voltage $\overline{V}_{I_{Ca}} = -11.5$ mV and $K = 7$ mV in mammalian cut skeletal fibers with 2 mM external $[Ca^{2+}]$ (Mejía-Alvarez et al., 1991). The difference in the values of central voltage is not surprising, given the differences in ionic media of the cell and bilayer experiments. The values of the steepness factor, revealing effective valences on the voltage sensors, should not be sensitive to the ionic environment and are identical.

In summary, our approach with the present bilayer experiments allowed for a description of voltage-dependent gating at both the single channel and macroscopic level. At the microscopic level, the opening of the channels was shown to be strictly voltage-dependent, and fast open channel events that were not previously resolved were separated from the noise by virtue of their voltage dependence. At the macroscopic level, we confirmed the existence of voltage-dependent inactivation in the absence of Ca^{2+} ions and improved the existing descriptions of the kinetics of activation and deactivation.

The results obtained with the present approach provide a framework for interpretation of events observed in further studies. In the second paper (Mundiña-Weilenmann et al., 1991) we report that cAMP-dependent protein kinase (protein kinase A) induces changes in both the kinetics and voltage dependence of gating of the Ca channels. Other interventions currently under investigation have been shown to modify these properties, including the *cis* addition of skeletal muscle ryanodine receptor protein (Ma et al., 1991) and specific pulsing patterns (J. Ma, et al., unpublished data).

We thank Dr. Ivan Stavrovsky for assistance in data analysis, Dr. Fred Cohen for comments and suggestions on the manuscript and Ms. Lucille Vaughn for word processing.

This work was supported by grants from National Institutes of Health (AR32808) to Eduardo Ríos, (HL23306) to M. Marlene Hosey, and by a grant from Muscular Dystrophy Association to Eduardo Ríos. Jianjie Ma and Cecilia Mundiña-Weilenmann are recipients of Muscular Dystrophy Association postdoctoral fellowships.

Received for publication 3 January 1991 and in final form 17 April 1991.

REFERENCES

Affolter, H., and R. Coronado. 1985. Agonist Bay K 8644 and CGP-28392 open calcium channels reconstituted from skeletal muscle transverse tubules. *Biophys. J.* 48:341–347.

Almers, W., R. Fink, and P. T. Palade. 1981. Calcium depletion in frog muscle tubules: the decline of calcium current under maintained depolarization. *J. Physiol.* 312:177–207.

Almers, W., and P. T. Palade. 1981. Slow calcium and potassium currents across frog muscle membrane: measurements with a vaseline-gap technique. *J. Physiol.* 312:159–176.

Alvarez, O., and R. Latorre. 1978. Voltage-dependent capacitance in lipid bilayers made from monolayers. *Biophys. J.* 21:1–17.

Avila-Sakar, A. J., G. Cota, R. Gamboa-Aldeco, J. García, M. Huerta, J. Muñiz, and E. Stefani. 1986. Skeletal muscle Ca^{2+} channels. *J. Muscle Res. Cell Motil.* 7:291–298.

Bean, B. P. 1989. Classes of calcium channels in vertebrate cells. *Annu. Rev. Physiol.* 51:367–384.

Bechem, M., and M. Schramm. 1988. Electrophysiology of dihydropyridine calcium agonists. *In* The Calcium Channel: Structure, Function and Implications. M. Morad, W. Nayler, S. Kazda, and M. Schramm, editors. Springer-Verlag, Berlin. 63–70.

Bickel, P. J., and K. A. Doksum. 1977. Mathematical Statistics: Basic Ideas and Selected Topics. Holden-Day Inc., Oakland, CA.

Campbell, K. P., A. T. Leung, and A. H. Sharp. 1988. The biochemistry and molecular biology of the dihydropyridine-sensitive calcium channel. *Trends Neurosci.* 11:425–430.

Cavalié, A., D. Pelzer, and W. Trautwein. 1986. Fast and slow gating behavior of single calcium channels in cardiac cells. Relation to activation and inactivation of calcium channel current. *Pfluegers Arch. Eur. J. Physiol.* 406:241–258.

Cleland, W. W. 1977. The statistical analysis of enzyme kinetic data. *Adv. Enzymol. Relat. Areas Mol. Biol.* 29:1–32.

Cognard, C., G. Romey, J.-P. Galizzi, M. Fosset, and M. Lazdunski. 1986. Dihydropyridine-sensitive Ca channels in mammalian skeletal muscle cells in culture: electrophysiological properties and interactions with Ca channel activator (Bay K 8644) and inhibitor (PN200-110). *Proc. Natl. Acad. Sci. USA.* 83:1518–1522.

Colquhoun, D., and F. J. Sigworth. 1983. Fitting and statistical analysis of single channel records. *In* Single Channel Recording. Plenum Publishing Corp., New York. 191–263.

Cota, G., and E. Stefani. 1989. Voltage-dependent inactivation of slow calcium channels in intact twitch muscle fibers of the frog. *J. Gen. Physiol.* 94:937–951.

Donaldson, P. L., and K. G. Beam. 1983. Calcium currents in a fast-twitch skeletal muscle of the rat. *J. Gen. Physiol.* 82:449–468.

Flockerzi, V., H.-J. Oeken, F. Hofmann, D. Pelzer, A. Cavalie, and W. Trautwein. 1986. Purified dihydropyridine-binding site from skeletal muscle t-tubules is a functional calcium channel. *Nature (Lond.).* 323:66–68.

Fosset, M., E. Jaimovich, E. Delpont, M. Lazdunski. 1983. [3H]Nitrendipine receptors in skeletal muscle. *J. Biol. Chem.* 258:6086–6092.

Francini, F., and E. Stefani. 1989. Decay of the slow calcium current in twitch muscle fibers of the frog is influenced by intracellular EGTA. *J. Gen. Physiol.* 94:953–969.

Galizzi, J. P., M. Fosset, and M. Lazdunski. 1984. Properties of receptors for the Ca channel blocker verapamil in transverse tubule membranes of skeletal muscle. *Eur. J. Biochem.* 144:211–214.

Glossmann, H., D. R. Ferry, and C. B. Boschek. 1983. Purification of the putative calcium channel from skeletal muscle with the aid of [^{3}H]nimodipine binding. *Naunyn Schmiedeberg's Arch. Pharmacol.* 323:1–11.

Glossmann, H., and J. Striessnig. 1990. Molecular properties of calcium channels. *Rev. Physiol Biochem. Pharmacol.* 114:1–105.

Hess, P., J. B. Lansman, and R. W. Tsien. 1984. Different modes of Ca channel gating behavior favored by dihydropyridine Ca agonist and antagonists. *Nature (Lond.).* 311:538–544.

Hosey, M. M., and M. Lazdunski. 1988. Calcium channels: molecular pharmacology, structure and regulation. *J. Membr. Biol.* 104:81–106.

Hui, C. S., and W. K. Chandler. 1990. Intramembrane charge movement in frog cut twitch fibers mounted in a double vaseline gap chamber. *J. Gen. Physiol.* 96:257–297.

Kokubun, S., and H. Reuter. 1984. Dihydropyridine derivatives prolong the open state of Ca channels in cultured cardiac cells. *Proc. Natl. Acad. Sci. USA.* 81:4824–4827.

Lamb, G. D., and T. Walsh. 1987. Calcium currents, charge movement and dihydropyridine binding in fast- and slow-twitch muscles of rat and rabbit. *J. Physiol.* 393:595–617.

Ma, J., and R. Coronado. 1988. Heterogeneity of conductance states in calcium channels of skeletal muscle. *Biophys. J.* 53:387–395.

Ma, J., M. M. Hosey, and E. Ríos. 1991. Skeletal muscle dihydropyridine and ryanodine receptor proteins interact in planar bilayers. *Biophys. J.* 59:201*a*. (Abstr.)

Markwardt, F., and B. Nilius. 1988. Modulation of Ca channel currents in guinea-pig single ventricular heart cells by the dihydropyridine Bay K 8644. *J. Physiol. (Lond.).* 399:559–575.

Meissner, G. 1984. Adenine nucleotide stimulation of Ca-induced Ca release in sarcoplasmic reticulum. *J. Biol. Chem.* 259:2365–2374.

Mejia-Alvarez, R., M. Fill, and E. Stefani. 1991. Voltage-dependent inactivation of t-tubular skeletal calcium channels in planar lipid bilayers. *J. Gen. Physiol.* 97:393–412.

Mikami, A., K. Imoto, T. Tanabe, T. Niidome, Y. Mori, H. Takeshima, S. Narumiya, and S. Numa. 1989. Primary structure and functional expression of the cardiac dihydropyridine-sensitive calcium channel. *Nature (Lond.).* 340:230–233.

Mundiña-Weilenmann, C., J. Ma, M. M. Hosey, and E. Rios. 1991. Dihydropyridine sensitive skeletal muscle Ca channels in polarized planar bilayers. 2. Effects of phosphorylation by cAMP-dependent protein kinase. *Biophys. J.* 60:000–000.

Ríos, E., and G. Brum. 1987. Involvement of dihydropyridine receptors in excitation-contraction coupling in skeletal muscle. *Nature (Lond.).* 325:717–720.

Rosemblatt, M., C. Hidalgo, C. Vergara, and N. Ikemoto. 1981. Immunological and biochemical properties of transverse tubule membranes isolated from rabbit skeletal muscle. *J. Biol. Chem.* 256:8140–8148.

Rosenberg, R. L., P. Hess, J. Reeves, H. Smilowitz, and R. W. Tsien. 1986. Calcium channels in planar lipid bilayers: new insights into the mechanisms of permeation and gating. *Science (Wash. DC).* 231:1564–1566.

Rosenberg, R. L., P. Hess, and R. W. Tsien. 1988. Cardiac calcium channels in planar lipid bilayers. L-type channels and calcium-permeable channels open at negative membrane potentials. *J. Gen. Physiol.* 92:27–54.

Sánchez, J. A., and E. Stefani. 1983. Kinetic properties of calcium channels of twitch muscle fibers of the frog. *J. Physiol.* 337:1–17.

Sanguinetti, M. C., D. S. Krafte, and R. S. Kass. 1986. Voltage-dependent modulation of Ca channel current in heart cells by Bay K 8644. *J. Gen. Physiol.* 88:369–392.

Scarborough, J. B. 1966. Numerical Mathematical Analysis, 6th edition. The Johns Hopkins Press, Baltimore, MD.

Schwartz, L. M., E. W. McCleskey, and W. Almers. 1985. Dihydropyridine receptors in muscle and voltage-dependent but most are not functional calcium channels. *Nature (Lond.).* 314:747–751.

Smith, J. S., E. J. Mckenna, J. Ma, J. Vilven, P. L. Vaghy, A. Schwartz, and R. Coronado. 1987. Calcium channel activity in a purified 1,4 dihydropyridine receptor preparation of skeletal muscle. *Biochemistry.* 26:7182–7188.

Talvenheimo, J. A., J. F. Worley, and M. T. Nelson. 1987. Heterogeneity of calcium channels from a purified dihydropyridine receptor preparation. *Biophys. J.* 52:891–899.

Tanabe, T., H. Takeshima, A. Mikami, V. Flockerzi, H. Takahashi, K. Kangawa, M. Kojima, H. Matsuo, T. Hirose, and S. Numa. 1987. Primary structure of the receptor for calcium channel blockers from skeletal muscle. *Nature (Lond.).* 328:313–318.

Tanabe, T., K. G. Beam, J. A. Powell, and S. Numa. 1988. Restoration of excitation-contraction coupling and slow calcium current in dysgenic muscle by dihydropyridine receptor complementary DNA. *Nature (Lond.).* 336:134–139.

Tanabe, T., K. G. Beam, B. A. Adams, T. Niidome, and S. Numa. 1990. Regions of the skeletal muscle dihydropyridine receptor critical for excitation-contraction coupling. *Nature (Lond.).* 346:567–569.